Significant elastic anisotropy in $Ti_{1-x}Al_xN$ alloys

Ferenc Tasnádi, Igor Abrikosov, Lina Rogström, Jonathan Almer,
Mats Johansson and Magnus Odén

Original Publication:

Ferenc Tasnádi, Igor Abrikosov, Lina Rogström, Jonathan Almer, Mats Johansson and Magnus Odén, Significant elastic anisotropy in $Ti_{1-x}Al_xN$ alloys, 2010, Applied Physics Letters, (97), 23, 231902-231904.
http://dx.doi.org/doi:10.1063/1.3524502

Significant elastic anisotropy in $Ti_{1-x}Al_xN$ alloys

Ferenc Tasnádi,[1,a)] Igor A. Abrikosov,[1] Lina Rogström,[1] Jonathan Almer,[2] Mats P. Johansson,[1] and Magnus Odén[1]
[1]*Department of Physics, Chemistry and Biology (IFM), Linköping University, Linköping SE-581 83, Sweden*
[2]*Advanced Photon Source, Argonne National Laboratory, Argonne, Illinois 60439, USA*

(Received 18 October 2010; accepted 16 November 2010; published online 6 December 2010)

Strong compositional-dependent elastic properties have been observed theoretically and experimentally in $Ti_{1-x}Al_xN$ alloys. The elastic constant, C_{11}, changes by more than 50% depending on the Al-content. Increasing the Al-content weakens the average bond strength in the local octahedral arrangements resulting in a more compliant material. On the other hand, it enhances the directional (covalent) nature of the nearest neighbor bonds that results in greater elastic anisotropy and higher sound velocities. The strong dependence of the elastic properties on the Al-content offers new insight into the detailed understanding of the spinodal decomposition and age hardening in $Ti_{1-x}Al_xN$ alloys. © *2010 American Institute of Physics*. [doi:10.1063/1.3524502]

TiAlN coatings are today used as wear protection, for example cutting tools. The alloy has cubic B1 structure and shows a combination of good oxidation resistance and superior mechanical properties at elevated temperatures as compared to TiN.[1] The good high temperature behavior is correlated with an isostructural spinodal decomposition of the $Ti_{1-x}Al_xN$ solid solution into coherent cubic Al- and Ti-enriched $Ti_{1-x}Al_xN$ domains that results in a hardness enhancement, i.e., age hardening, at 800–1000 °C.[2–4] Several subsequent studies have highlighted different aspects of importance for the understanding of the decomposition and stability of this materials system, such as the influence of nitrogen off-stoichiometry,[5] pressure,[6] and domain growth behavior.[7]

Although the phase stability and performance of $Ti_{1-x}Al_xN$ coatings has attracted much attention, little is known on the fundamental aspect of their elastic properties. This is so even though it is known that the for example spinodal decomposition is influenced by elastic anisotropy[8] as well as the hardness enhancement observed relies on a shear modulus difference between the formed domains.[9] In this work we model the influence of composition x in the $Ti_{1-x}Al_xN$ system on the elastic constants and elastic anisotropy theoretically with first-principles density-functional theory (DFT) and compare the obtained results with experimentally recorded anisotropy. The good correlation between our theoretical and experimental results suggests that the elastic properties are strongly affected by the composition, which is to date and overlooked parameter for tailoring the properties of hard coatings.

The special quasirandom structure (SQS) method[10] has been applied to model the alloys. The approximate SQS supercells were generated by optimizing the Warren–Cowley pair short-range order (SRO) parameters[11] up to the seventh neighboring shell by applying the Metropolis-type simulated annealing algorithm with a cost-function built from the properly weighted pair SRO parameters. Substitutional alloys have been considered, where the Al atoms can occupy sites only on the Ti-sublattice. Accordingly, the SRO parameters were calculated only on the Ti-sublattice. Among the generated SQS supercells, the ones with size of $(4\times4\times3)$ have proved to be good approximations of random alloys over the entire composition range. This size means altogether 96 atoms in the supercell. The elastic constants of the SQS supercells were obtained by first-principles total energy calculations within DFT using the projector augmented wave approach[12] as implemented in the Vienna *ab initio* simulation package.[13] The Perdew–Burke–Ernzerhof generalized gradient approximation[14] of the exchange-correlation energy functional with a kinetic energy cutoff of 450 eV has been applied. Integrations over the Brillouin zone employed a $6\times6\times6$ grid of special k points. The elastic stiffness constants were derived by finite difference technique from the second order Taylor-expansion coefficients of the total energy.

Figure 1 presents the obtained *ab initio* cubic elastic constants, C_{11}, C_{12}, and C_{44}, of $Ti_{1-x}Al_xN$ alloys as a function of Al-content. The constants change smoothly and C_{12} and C_{44} increase with the amount of Al, while C_{11}, in comparison, shows a pronounced decrease. The increase of C_{44} has been theoretically observed in supercell calculations for $Ti_{1-x}Al_xN$.[15]

These facts have important implications on the general elastic behavior of the alloy, as the longitudinal sound veloc-

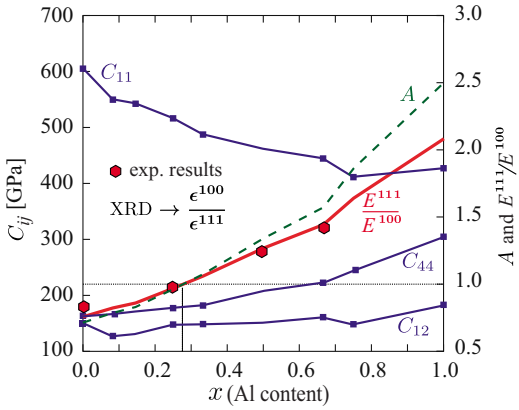

FIG. 1. (Color online) The calculated elastic stiffness constants, C_{11}, C_{12}, and C_{44}, of $Ti_{1-x}Al_xN$ alloys and the extracted theoretical and experimental values of Young's modulus ratio, E^{111}/E^{100}. The dashed line shows Zener's elastic anisotropy factor, $A=2C_{44}/(C_{11}-C_{12})$.

a)Electronic mail: tasnadi@ifm.liu.se.

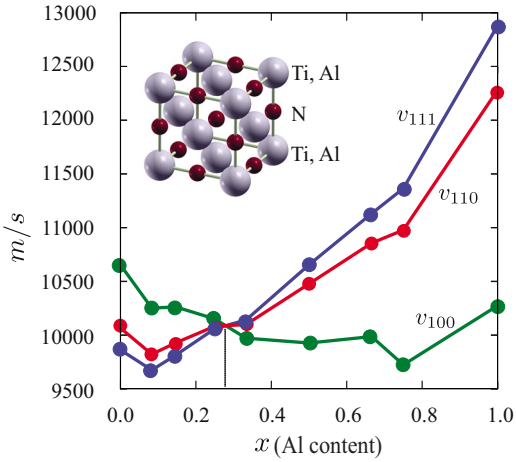

FIG. 2. (Color online) Longitudinal sound velocities in directions [100], [110], and [111], extracted from $\rho v_{100}^2 = C_{11}$, $\rho v_{110}^2 = (1/2)(C_{11}+C_{12}+2C_{44})$, $\rho v_{111}^2 = (1/3)(C_{11}+2C_{12}+4C_{44})$, where ρ is the density.

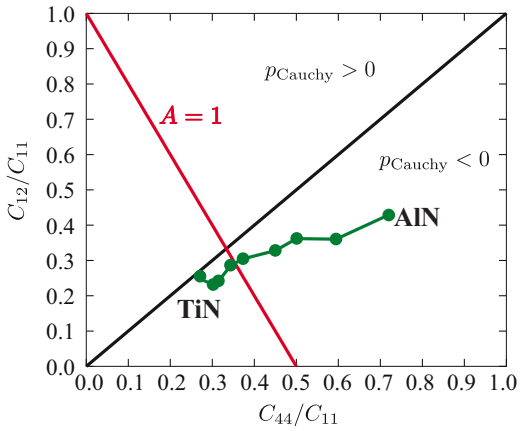

FIG. 3. (Color online) Blackman's diagram of TiAlN alloys.

ity is then expected to decrease in the [100] direction and increase along [111]. The extracted theoretical longitudinal sound velocities v_{hkl}, shown in Fig. 2, indicate elastically isotropic $Ti_{1-x}Al_xN$ at $x \approx 0.28$. The directional anisotropy of the longitudinal sound velocities indicate significant difference in the nature of the nearest neighbor bonds with increasing Al-content. The strong increase of v_{111} is unambiguously connected to the increasing C_{44} in Fig. 1, while the decrease of v_{100} is a clear consequence of the softening of C_{11}, particularly at low Al-content.

To quantify the elastic anisotropy in this system, we invoke Zener's elastic- shear anisotropy index, $A = 2C_{44}/(C_{11} - C_{12})$.[16] Most of the materials show elastic anisotropy by having $A \neq 1$, but in particular cases the condition of isotropy $A = 1$ can be fulfilled. Though one never or only rarely expects elastic isotropy for compounds, the compositional freedom of alloys allows for isotropic elastic behavior at a certain concentration, here around $x \approx 0.28$, see Fig. 1.

To verify the predicted elastic behavior, arc evaporated $Ti_{1-x}Al_xN$ coatings with the composition $x = 0$, 0.25 ± 0.02, 0.50 ± 0.02, and 0.67 ± 0.02 (determined by energy dispersive x-ray analysis) were deposited. The synthesis was conducted in a deposition chamber (Sulzer Metaplas MZR323) using $Ti_{1-x}Al_x$ alloy targets, a 2 Pa N_2 reactive atmosphere and a bias potential of -20 V. The depositions were performed at ≈ 200 °C on WC/Co substrates [Seco Tools HX, chemical composition (wt %) WC 94Co 6] of size $13 \times 13 \times 4$ mm^3 and hardness 1635 HV10. The 8 μm thick coatings are dense and exhibit columnar growth that results in an isotropic microstructure within the film plane. More details on the coating microstructure can be found elsewhere.[2,3,7]

Analysis was performed using high-energy ($E = 80.72$ keV) synchrotron x-ray diffractometry at beamline 1-ID at the Advanced Photon Source (APS), Illinois USA. The beam was vertically focused using refractive lenses to 1.5 μm (full-width-half-maximum) while the horizontal size was defined to 100 μm using slits. An ion chamber in front of the specimen was used to measure incident beam intensity and a 2048×2048 area detector (GE Angio) with 200×200 μm^2 pixels was placed 2250 mm downstream from the sample. The samples were sectioned to a 1 mm thick slice, such that diffraction data were recorded in transmission mode. Each detector exposure consisted of Debye rings 111 and 200 from the cubic B1 structure, which were corrected for detector dark-field current. The strains in the as deposited samples were determined through a procedure outlined elsewhere.[17] An alumina powder was used to calibrate the detector distance and tilt angles resulting in an accuracy of the strain determination to better than 10^{-4}. The biaxial stress, σ, known to be generated during growth[18] results in strain partitioning among the grains[19] depending on their crystallographic orientation. Hence, $\sigma = E^{hkl}\epsilon^{hkl}$, where E^{hkl} and ϵ^{hkl} are the elastic (Young's) modulus and strain of the grains contributing to the diffraction signal having a crystallographic direction $\langle hkl \rangle$ oriented perpendicular to the growth direction, i.e., we assume Reuss strain distribution. The Reuss model has previously been applied to sufficiently well describe the strain distribution in arc evaporated transition nitrides.[17] Accordingly, a measure of the elastic anisotropy can be experimentally determined by the strain ratio $\epsilon_{111}/\epsilon_{200} = E_{200}/E_{111}$ and since $E_{200} = E_{100}$, comparison between calculated elastic modulus and measured strain can be made. Such comparison is given in Fig. 1 where the calculated elastic modulus ratio and measured strain ratio are plotted as a function of Al-content. The close agreement between measured and calculated elastic anisotropy confirms the validity of the calculations.

Based on *ab initio* supercells calculations of TiAlN, Mayrhofer[15] extracted C_{44} and suggested that its variation with Al-content was related to the bonding in their model. To further study the interatomic bonding in our modeling of quasirandom solid solution cubic $Ti_{1-x}Al_xN$ alloys, we plot the data in the form of Blackman's diagram[20] in Fig. 3.

Such diagram plots the ratios of elastic constants, C_{12}/C_{11} versus C_{44}/C_{11}, and reveals general characteristics of the system, such as elastic anisotropy and interatomic bonding type. With the help of this diagram one can determine the change in the character of bonding with composition. The 45° solid line represents the Cauchy relationships, $C_{12} = C_{44}$, or zero Cauchy pressure. According to Pettifor[21] the Cauchy pressure, $C_{12} - C_{44}$, is positive in case of fairly metallic bonds and negative for more directional or covalentlike bonds. $Ti_{1-x}Al_xN$ alloys are all in the covalentlike region. The decreasing Cauchy pressure with increasing Al-content indicates a tendency toward stronger covalent character of the bonds, which in general results in increased resistance against shearing and thus in increasing C_{44}. The increasing longitudinal sound velocity v_{111} indicates also an increasing covalent nature of the system. A longitudinal

wave along [111] affects the six nearest neighbor bond angles between the N–(Ti,Al)–N layers, as depicted in the inset of Fig. 2. Thus, the increased v_{111} results from an increased resistance to bending of these six bonds, which is a clear indication of the increased covalent nature of the nearest neighbor bonds. The decrease of C_{11} correlates to the decreasing bulk modulus with increasing Al-content. Thus, the more compliant nature of C_{11} can be understood as weakening of the average bond strength in the local octahedral arrangements of the B1 structure. This agrees with the obtained rapid initial decrease of v_{100}. Consequently, an increased Al-content changes the bonding nature of $Ti_{1-x}Al_xN$ alloys in two different senses. Although the bonds become more directional, the average strength between the octahedrally arranged atoms gets slightly weaker. Furthermore, the observed directional anisotropy should establish an anisotropic strain distribution in the different crystallographic directions.

The strong dependency of the elastic properties on the Al-content presented here offers new insight to the detailed understanding of the observed age hardening in $Ti_{1-x}Al_xN$ alloys as an effect of spinodal decomposition. First, the nature of the $Ti_{1-x}Al_xN$ decomposition and resulting microstructure are affected by the elastic anisotropy, which was already pointed out by, e.g., Cahn.[22] Second, as the Ti- and Al-rich domains evolve during spinodal decomposition the spatially fluctuating elastic properties will give rise to a Koehler[9] type hardening in addition to strengthening due to the coherency strains between the domains. Its origin is the differences in elastic shear modulus, giving rise to repelling shear stresses acting on dislocations gliding across the compositional gradients. The validity of this model has been demonstrated on multilayers by for example by Chu *et al.*[23] for several different material systems as long as the composition modulation period is less than approximately 20 nm. Hence, we conclude that the observed age hardening seen for TiAlN (Ref. 4) and TiN/TiAlN multilayers[24] are affected by evolving elastic properties and this detailed understanding can be utilized to tailor material properties, such as hardness and thermomechanical response of $Ti_{1-x}Al_xN$ alloys.

This work was supported by the SSF project Designed Multicomponent coatings, MultiFilms and the Swedish Research Council (VR). Use of the Advanced Photon Source was supported by the U.S. Department of Energy, Office of Science, Office of Basic Energy Sciences under Contract No. DE-AC02-06CH11357. Calculations have been performed at Swedish National Infrastructure for Computing (SNIC).

[1] A. Hörling, L. Hultman, M. Odén, J. Sjölén, and L. Karlsson, Surf. Coat. Technol. **191**, 384 (2005).
[2] A. Hörling, L. Hultman, M. Odén, J. Sjölén, and L. Karlsson, J. Vac. Sci. Technol. A **20**, 1815 (2002).
[3] A. Knutsson, M. P. Johansson, P. O. A. Persson, L. Hultman, and M. Odén, Appl. Phys. Lett. **93**, 143110 (2008).
[4] P. H. Mayrhofer, A. Hörling, L. Karlsson, J. Sjölén, T. Larsson, C. Mitterer, and L. Hultman, Appl. Phys. Lett. **83**, 2049 (2003).
[5] B. Alling, A. Karimi, L. Hultman, and I. A. Abrikosov, Appl. Phys. Lett. **92**, 071903 (2008).
[6] B. Alling, M. Odén, L. Hultman, and I. A. Abrikosov, Appl. Phys. Lett. **95**, 181906 (2009).
[7] M. Odén, L. Rogström, A. Knutsson, M. R. Terner, P. Hedström, J. Almer, and J. Ilavsky, Appl. Phys. Lett. **94**, 053114 (2009).
[8] D. Seol, Acta Mater. **51**, 5173 (2003).
[9] J. Koehler, Phys. Rev. B **2**, 547 (1970).
[10] A. Zunger, S. Wei, L. Ferreira, and J. Bernard, Phys. Rev. Lett. **65**, 353 (1990).
[11] A. V. Ruban and I. A. Abrikosov, Rep. Prog. Phys. **71**, 046501 (2008).
[12] P. E. Blöchl, Phys. Rev. B **50**, 17953 (1994).
[13] G. Kresse and J. Furthmüller, Phys. Rev. B **54**, 11169 (1996).
[14] J. P. Perdew, K. Burke, and M. Ernzerhof, Phys. Rev. Lett. **77**, 3865 (1996).
[15] P. H. Mayrhofer, D. Music, and J. M. Schneider, J. Appl. Phys. **100**, 094906 (2006).
[16] J. F. Nye, *Physical Properties of Crystals: Their Representation by Tensors and Matrices* (Oxford University Press, New York, 1985).
[17] J. Almer, U. Lienert, R. L. Peng, C. Schlauer, and M. Oden, J. Appl. Phys. **94**, 697 (2003).
[18] J. Almer, M. Oden, and G. Hakansson, Thin Solid Films **385**, 190 (2001).
[19] P. Hedström, T.-S. Han, U. Lienert, J. Almer, and M. Odén, Acta Mater. **58**, 734 (2010).
[20] M. Blackman, Proc. R. Soc. London, Ser. A **164**, 62 (1938).
[21] D. G. Pettifor, Mater. Sci. Technol. **8**, 5 (1992).
[22] J. Cahn, Acta Metall. **9**, 795 (1961).
[23] X. Chu and S. A. Barnett, J. Appl. Phys. **77**, 4403 (1995).
[24] A. Knutsson, M. P. Johansson, L. Karlsson, and M. Odén, J. Appl. Phys. **108**, 044312 (2010).